

Phase behavior of bent-core molecules

Yves Lansac, Prabal K. Maiti,* Noel A. Clark, and Matthew A. Glaser

Condensed Matter Laboratory, Department of Physics, and Ferroelectric Liquid Crystal Materials Research Center,
University of Colorado, Boulder, Colorado 80309

(Received 26 August 2002; published 28 January 2003)

Recently, a new class of smectic liquid crystal phases characterized by the spontaneous formation of macroscopic chiral domains from achiral bent-core molecules has been discovered. We have carried out Monte Carlo simulations of a minimal hard spherocylinder dimer model to investigate the role of excluded volume interactions in determining the phase behavior of bent-core materials and to probe the molecular origins of polar and chiral symmetry breaking. We present the phase diagram of hard spherocylinder dimers of length-diameter ratio of 5 as a function of pressure or density and dimer opening angle ψ . With decreasing ψ , a transition from a nonpolar to a polar smectic *A* phase is observed near $\psi=167^\circ$, and the nematic phase becomes thermodynamically unstable for $\psi<135^\circ$. Free energy calculations indicate that the antipolar smectic *A* (SmAP_A) phase is more stable than the polar smectic *A* phase (SmAP_F). No chiral smectic or biaxial nematic phases were found.

DOI: 10.1103/PhysRevE.67.011703

PACS number(s): 61.30.Cz, 64.70.Md

I. INTRODUCTION

Molecular chirality plays an important role in the science of liquid crystals (LCs), leading to cholesteric LCs [1], blue phases [2], ferroelectric [3] and antiferroelectric [4] smectic phases, and twist grain boundary phases [5]. In all of these examples, chirality is an intrinsic property built into the chemical structure of the LC molecules. Recently, a new class of smectic LC phases (SmCP phases) characterized by the spontaneous formation of macroscopic chiral layers from achiral molecules has been discovered [6,7]. The molecules comprising these phases have “bow” or “banana” shaped cores. The resulting phases exhibit two spontaneous symmetry-breaking transitions: polar molecular orientational ordering within the layer plane, and molecular tilt, which together produce chiral layers with a handedness that depends on the direction of the tilt relative to the polar axis. Very large second-order nonlinear optical (NLO) coefficients have been measured in the ferroelectric state of such materials, bearing some promising applications in NLO devices [8,9].

From a theoretical point of view, the relationship of phase behavior to the specific bent-core molecular shape is of fundamental interest. In this paper, we investigate a minimal excluded volume model of bent-core mesogens, focusing on the molecular origins of polar and/or chiral symmetry breaking. Of particular interest is the coupling between polar and chiral symmetry breaking. In most bent-core materials studied to date, polar symmetry breaking is accompanied by chiral symmetry breaking induced by molecular tilt. This empirical fact, and recent phenomenological studies [10,11], raise the question whether there is a fundamental connection between polarity and chirality in molecular fluids. However, an *untitled* polar smectic (SmAP_A) phase has recently been reported [12], demonstrating that polar ordering can be present in the absence of chiral ordering in bent-core liquid

crystal materials. Another empirical observation is that bent-core materials exhibiting SmCP phases generally do not exhibit nematic phases, although two exceptions have recently been reported [13,14]. One objective of this study is to establish the molecular shape requirements for the occurrence of the nematic phase in bent-core materials. Finally, we explore the possibility of *biaxial* nematic ordering in bent-core materials, motivated by recent experimental [14,15] and theoretical [16] indications.

Hard-core models are particularly appealing due to their simplicity and relative ease of computation, both in simulation and theory. In particular, hard spherocylinders have been widely studied as simple models for conventional LCs [17,18]. This model exhibits rich phase behavior including isotropic, nematic, smectic, columnar, and solid phases, the phase transitions being driven by the competition of two main entropic contributions, the orientational entropy favoring the isotropic phase and the positional entropy favoring ordered phases, as shown in the 1940s by Onsager in the limit of infinitely thin rods [19].

II. MODEL

To capture the main characteristics of the collective behavior of bent-core molecules, we extend the spherocylinder model by introducing a hard-core dimer formed by two interdigitated hard-core spherocylinders sharing one spherical end cap (see inset in Fig. 1). This is an ideal model system to consider due to the relatively small parameter space. There are three parameters: two geometrical parameters, namely, the length-to-breadth ratio L/D , where L and D are, respectively, the length and diameter of each spherocylinder, and the opening angle ψ between the two spherocylinder axes; and one thermodynamic parameter, the reduced pressure P^* , defined as $P^* = \beta P v_o$ or, equivalently, the reduced density ρ^* defined as $\rho^* = \rho v_o$. Here, v_o is the volume of the equivalent straight hard spherocylinder ($\psi=180^\circ$), $v_o = \pi D^3/6 + \pi L' D^2/4$, with $L' = 2L$. In all the simulations presented below, we consider a single value for the length-to-breadth ratio, namely, $L/D = 5$. This ratio has been chosen

*Present address: Beckman Institute, California Institute of Technology, 400 South Wilson Avenue, Pasadena, CA 91125.

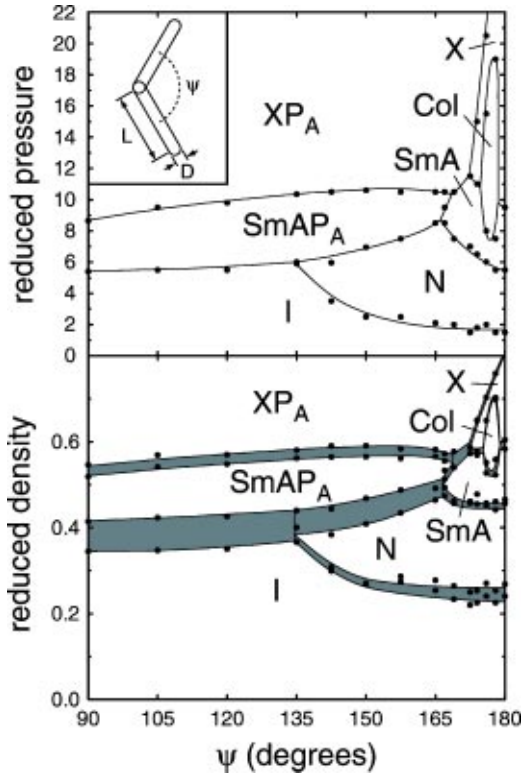


FIG. 1. Phase diagram of spherocylinder dimers (inset) with aspect ratio $L/D=5$ as a function of opening angle ψ and reduced pressure P^* (top) and reduced density ρ^* (bottom). All two-phase regions are shaded. The following phases are present: isotropic liquid (I), nematic (N), polar smectic A ($SmAP_A$), smectic A (SmA), columnar (Col), polar crystal (XP_A), and crystal (X).

in order to roughly represent the equivalent geometrical envelope described by a realistic bow shaped molecule with fully extended aliphatic tails.

Using a similar model, Camp *et al.* [20] have found a nematic phase and a smectic A phase for bent-core molecules roughly half as long as the ones considered here. However, no systematic study of the phase behavior was carried out. Recently, a polar smectic A phase and a chiral crystal phase have been observed for a “polybead” model of bent-core molecules with an opening angle of $\psi=140^\circ$ [21], and polar smectic A and nematic phases have been reported for a system of banana-shaped Gay-Berne dimers with an opening angle of $\psi=140^\circ$ [22].

To investigate the phase behavior of our model as a function of the pressure and of the opening angle ψ , we perform N - P - T Monte Carlo (MC) simulations, with periodic boundary conditions, on a system of $N=400$ bent-core molecules. For each opening angle, the system is initially prepared at high pressure in the close-packed fcc-like crystal phase corresponding to the highest number density (antipolar crystal, see Fig. 2). The unit cell contains two molecules and is defined by the three lattice vectors $\mathbf{a}=D[1/\cos\theta,0,0]$, $\mathbf{b}=D[1/(2\cos\theta),\sqrt{3}/2,0]$, $\mathbf{c}=D[0,0,4L/(D\cos\theta)+2\Delta z]$ with $\Delta z=\sqrt{39\cos^4\theta-6\cos^2\theta-1}/(4\sqrt{3}\cos^2\theta)$ and $\theta=(\pi-\psi)/2$. The positions of the apex of the molecules in a unit cell are $\mathbf{r}_1=D[0,0,0]$ and $\mathbf{r}_2=D[1/(2\cos\theta)$

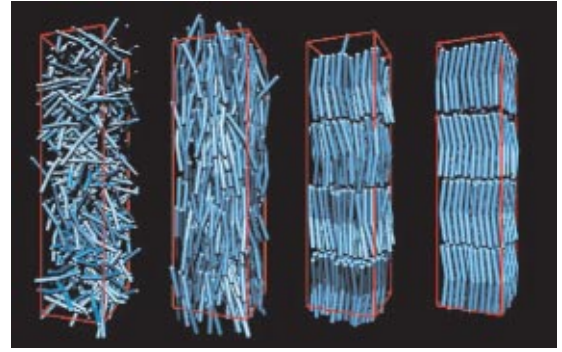


FIG. 2. (Color online only) Final configurations from Monte Carlo simulations of $N=400$ bent-core molecules with opening angle $\psi=165^\circ$ as a function of pressure. From left to right: isotropic phase ($P^*=1$), nematic phase ($P^*=5$), polar smectic A ($P^*=10$), and polar crystal ($P^*=15$).

$-2L/(D\sin\theta),\Delta y,2L/(D\cos\theta)+\Delta z]$ with $\Delta y=(3\cos^2\theta-1)/(4\sqrt{3}\cos^2\theta)$. The equation of state $P^*(\rho^*)$ is determined by measuring the density ρ^* as the pressure is decreased incrementally from the crystalline state. At each state point (ψ, P^*) , 2×10^5 MC cycles are used for equilibration and 1×10^6 MC cycles are used for production of the results.

The location of the phase boundaries is determined from the equation of state $P^*(\rho^*)$, and the nature of the coexisting phases is investigated through the computation of various order parameters. In-layer crystalline order is probed with the translational order parameters ρ_{Gk} defined as $\rho_{Gk}=(1/M)\sum_{j=1}^M\exp(i\mathbf{G}_k\cdot\mathbf{r}_j)$, where \mathbf{G}_1 , \mathbf{G}_2 and \mathbf{G}_3 are the reciprocal basis vector of a deformed hexagonal lattice, \mathbf{r}_j is the position of the center of mass of molecule j , and M is the number of molecules in a given layer. Smectic order is measured by the layer translational order parameter ρ_{\parallel} defined as $\rho_{\parallel}=(1/N)\sum_{j=1}^N\exp(i\mathbf{G}_{\parallel}\cdot\mathbf{r}_j)$ with $\mathbf{G}_{\parallel}=(2\pi/d)\hat{\mathbf{z}}$, where d is the layer spacing and $\hat{\mathbf{z}}$ is the layer normal. Polar orientational order is detected using the polar order parameter \mathbf{m} defined as $\mathbf{m}=(1/M)\sum_{j=1}^M\hat{\mathbf{m}}_j$, where $\hat{\mathbf{m}}_j$ is a unit vector contained in the plane of the molecule and passing through the apex of the molecule. Note that the polar order parameter defined here probes only polar ordering within each layer and does not discriminate between distinct relative orientations of the polar axis in adjacent layers. Finally, molecular orientational order is determined from the largest eigenvalue of the second-rank tensorial orientational order parameter $Q_{\alpha\beta}$, defined as $Q_{\alpha\beta}=(1/N)\sum_{j=1}^N(\frac{3}{2}n_{j\alpha}n_{j\beta}-\frac{1}{2}\delta_{\alpha\beta})$, where $\alpha,\beta=x,y,z$, and $\hat{\mathbf{n}}_j$ is a unit vector parallel to the molecular end-to-end vector for molecule j .

III. RESULTS

The (ψ, P^*) and (ψ, ρ^*) phase diagrams are presented in Fig. 1. Rich phase behavior is found, with isotropic (I), nematic (N), smectic A (SmA), polar smectic A ($SmAP_A$), columnar (Col), crystal (X), and polar crystal (XP_A) phases. Configurations from the isotropic, nematic, polar smectic and polar crystalline phases are shown in Fig. 2, for an opening angle of $\psi=165^\circ$.

The nematic phase is stable for opening angles larger than $\psi=135^\circ$. With decreasing opening angle, the region of stability of the nematic phase decreases, vanishing for opening angles smaller than $\sim 135^\circ$, leading to an (I, N, SmAP_A) triple point near $\psi=135^\circ$. It is interesting to note that for $L/D=2$ dimers, small opening angles seem to destabilize the smectic phase rather than the nematic phase [20]. Due to the weak coupling between adjacent layers in the polar smectic and crystal phases, it was impossible to determine the relative stability of polar and antipolar order by direct simulation. On the basis of free energy calculations for a single-state point in the SmAP phase described later in this section, we tentatively propose that the antipolar smectic A (SmAP_A) and antipolar crystal (XP_A) states are more thermodynamically stable than the polar smectic A (SmAP_F) and polar crystal (XP_F) states. Recently, a bent-core molecule with fluorine substitutions on the outer rings has been found to exhibit an antipolar smectic A phase (SmAP_A) [12].

The vast majority of bent-core materials exhibiting liquid crystal behavior, and in particular SmCP phases, have an opening angle between 120° and 135° , and do not exhibit any nematic phase. Quite interestingly, two classes of bent-core compounds having an opening angle between 134° and 148° [13,23] exhibit both smectic and nematic phases. These observations, in good qualitative agreement with the predictions of our model, tend to confirm the hypothesis that excluded volume interactions play a central role in the behavior of such materials.

The existence of a biaxial nematic phase remains an elusive possibility in thermotropic LCs. Due to their bent-core geometry, banana molecules are good candidates to exhibit such phenomena. Recent experiments suggest that the nematic phase exhibited by two classes of bent-core material might be biaxial [14,15]. Moreover, using a simplification of the Onsager second-virial treatment and bifurcation analysis, Teixeira *et al.* have found a biaxial nematic phase in the limit of very long bent-core molecules [16]. However, the nematic phase presented by our hard-core model does not exhibit any biaxiality. It is likely that the reported biaxiality is due to more subtle interactions and/or to the presence of the flexible tails. A biaxial nematic phase has been reported for $L/D=9.5$ hard spherocylinder dimers, but no transition from/to an isotropic liquid has been reported [20].

Because straight spherocylinders do not exhibit any polar smectic ordering, it is expected that our model should exhibit a transition from nonpolar smectic (SmA) to polar smectic (SmAP_A). This transition occurs for an opening angle between 167° and 169° , and is associated with two triple points, a $(\text{SmA}, \text{SmAP}_A, N)$ triple point near $\psi=167^\circ$ and a $(\text{SmA}, \text{SmAP}_A, \text{XP}_A)$ triple point near $\psi=169^\circ$. Very recently, the first group of bent-core molecules exhibiting both SmCP and a SmA (as well as SmC and nematic phases in one case) has been synthesized [13,24]. The opening angles measured by nuclear magnetic resonance techniques for the region of appearance of the smectic A are in the range 132° – 145° , but no polar order has been detected [25], lowering the upper limit of stability of a polar smectic phase with respect to our predictions.

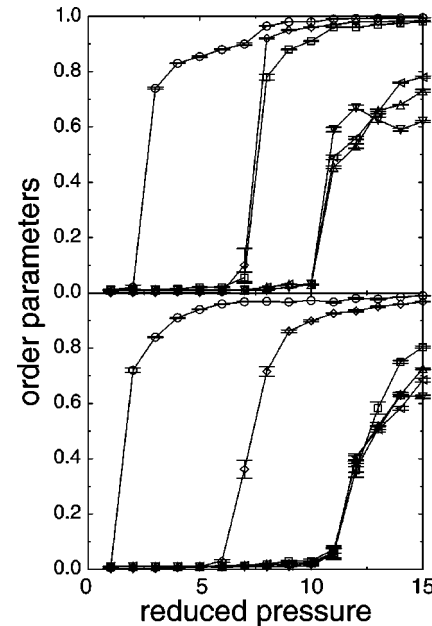


FIG. 3. Evolution of the squared magnitude of order parameters as a function of reduced pressure for opening angles of $\psi=157.5^\circ$ (top) and $\psi=172.5^\circ$ (bottom) showing, respectively, the phase sequences XP_A - SmAP_A - N - I and XP_A - SmA - N - I as a function of decreasing pressure. The following order parameters are plotted: (Δ , ∇ , \triangleleft) solid-liquid order parameters ρ_1 , ρ_2 , ρ_3 ; (\square) polar order parameter \mathbf{m} ; (\diamond) smectic order parameter $\rho_{||}$; (\circ) the largest eigenvalue of the nematic order parameter $Q_{\alpha\beta}$.

Figure 3 displays the evolution of the order parameters for opening angles $\psi=157.5^\circ$ and $\psi=172.5^\circ$. In the former case, a polar smectic phase characterized by a high value of both smectic and polar order parameters is present, while in the latter case the appearance of a smectic phase from the higher density crystal phase is accompanied by a jump to zero of both the crystal order parameters and the polar order parameter. The smectic phases (both polar and nonpolar) do not exhibit any tilt. Nevertheless, our results tend to confirm the hypothesis that the polar ordering is related to the distinctive bent-core shape of the molecules, but is not strongly related to the molecular tilt. Thus, polarity does not imply chirality in the minimal steric model presented here.

A transition between a polar crystalline phase and a narrow nonpolar crystalline phase (i.e., a rotator phase) is also present. This rotator phase is stable for opening angles larger than $\psi=172.5^\circ$, and is characterized by a $(\text{SmA}, X, \text{XP}_A)$ triple point around $\psi=172.5^\circ$. Quite interestingly, the rotator phase competes with a columnar phase for opening angles larger than $\psi=174^\circ$ and smaller than $\psi=180^\circ$. This narrow columnar phase is characterized by significant two-dimensional crystal order parameters but a negligible magnitude of the smectic order parameter. Since no clear evidence of such a phase was found for straight spherocylinders, a slightly bent molecular shape seems to stabilize the columnar phase. Due to the rather unexpected appearance of the columnar phase, we performed additional studies of this region of the phase diagram using helical periodic boundary conditions [26] for $N=400$ and a direct “quench” from a crystal-

line state to the middle of the columnar phase for $\psi=176^\circ$ with helical periodic conditions for a larger system ($N=1600$). A columnar phase was observed in both studies. However, we feel that free energy computations are needed in order to assess the relative thermodynamic stability of the columnar phase, the nonpolar smectic phase, and the rotator phase.

Insights into the shape of the phase boundaries can be gained by assuming, to a first approximation, that the partition function of the system can be decomposed into a product of positional and orientational contributions, in which case the entropy is the sum of an orientational entropy and a translational entropy. Competition between different forms of entropy determines the stability of a given phase at a given density. In the limit of straight spherocylinders, the isotropic-nematic phase transition occurs when the gain in positional entropy S^{pos} exceeds the loss of orientational entropy S^{orient} [19]. A nematic-smectic phase transition occurs when the gain in translational entropy perpendicular to the long molecular axis S_{\perp}^{pos} exceeds the loss of positional entropy parallel to the long molecular axis $S_{\parallel}^{\text{pos}}$, leading to the formation of a stack of two-dimensional liquid layers. Similar reasoning can be applied to bent-core molecules: in the range $134^\circ < \psi < 180^\circ$, the isotropic phase is more favorable at smaller opening angles. As the cores become more bent, the gain in positional entropy associated with nematic ordering is reduced, and the nematic phase range is reduced, eventually disappearing for $\psi < 134^\circ$. The shape of the nematic-SmAP_A boundary (i.e., for $134^\circ < \psi < 167^\circ$) can be qualitatively understood in the same way by noticing that the positional entropy parallel to the long molecular axis $S_{\parallel}^{\text{pos}}$ is larger for larger opening angles than for smaller ones, stabilizing the nematic phase for larger opening angles. This trend is reversed for the nematic-SmA transition (i.e., for $\psi > 167^\circ$) because the absence of polar order leads to jamming, reducing the translational entropy perpendicular to the long molecular axis S_{\perp}^{trans} for decreasing opening angles. This effect is responsible for the enhanced stability of the nematic phase for decreasing opening angles.

We turn now to the investigation of the nature of the polar smectic phase, more specifically to determine whether the polar or antipolar arrangement of adjacent layers is more thermodynamically stable.

Based on extensive quantum chemical and atomistic simulation studies of MHPOBC [27,28], we recently proposed that the entropy content of molecular-scale fluctuations of the interface between smectic *C* layers (“out-of-layer” molecular fluctuations) provides a general thermodynamic mechanism that uniquely favors synclinc ordering (a uniform tilt direction in all layers), and that the suppression of out-of-layer fluctuations in MHPOBC and similar materials, due to their unusual conformational behavior, permits the appearance of anticlinic ordering (a tilt direction that alternates from layer to layer) [29]. Evidence for a correlation between out-of-layer fluctuations and clinicity has been found previously by Fukuda and co-workers, who observed distinct higher-order Bragg reflections in x-ray diffraction measurements on several antiferroelectric liquid

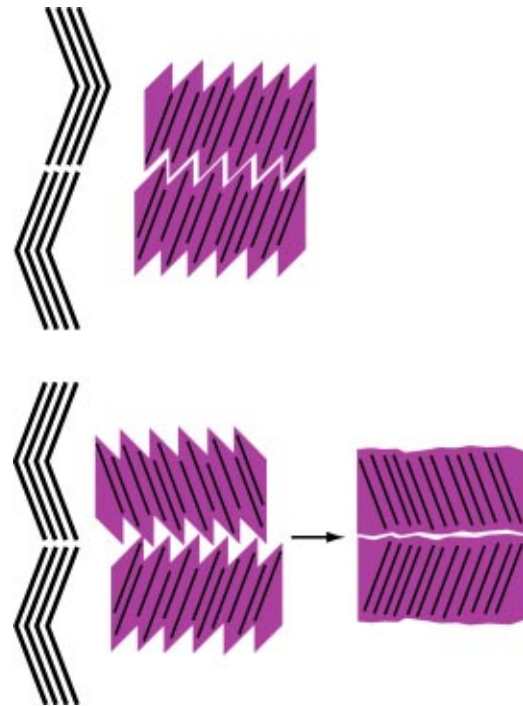


FIG. 4. Sawtooth model for rodlike molecules in synclinc smectic phase (top right) and anticlinic smectic phase (bottom right). The antipolar state of bent-core molecules (top left) exhibits synclinc layer interface while the polar state (bottom left) exhibits anticlinic layer interface. Thus, the sawtooth model predicts that the entropy associated with out-of-layer fluctuations should favor the antipolar state.

crystals [30]. Recently, we examined the general thermodynamic mechanism outlined above by assessing the contribution of molecular-scale interface fluctuations to the relative free energy of synclinc and anticlinic states of the hard spherocylinder system by means of Monte Carlo simulation [31].

The essence of this thermodynamic mechanism is captured by a simple conceptual model, the “sawtooth” model, shown schematically in Fig. 4. In this model, out-of-layer displacements of molecules in tilted smectic layers are assumed to impart a polar, or sawtooth, character to fluctuations of the layer interface (a necessary consequence of the symmetry of the interface). When two adjacent layers are tilted in the same direction, the sawteeth mesh, leading to an efficient filling of space. If adjacent layers are tilted in opposite directions, however, the sawteeth do not mesh, and space is not filled efficiently. Under constant volume conditions, the system fills space either by quenching out-of-layer fluctuations or by increasing the in-layer molecular density (or both). In either case, there is an entropic penalty (the entropy of the anticlinic state is lower than that of the synclinc state), so the entropy associated with out-of-layer fluctuations uniquely favors the synclinc state.

We extend this model to the case of hard bent-core molecules by noticing that at the interface between the SmAP layers, the antipolar state exhibits synclinc layer interfaces while the polar state exhibits an anticlinic layer interface (see Fig. 4). Therefore, the sawtooth model predicts that the an-

tipolar state should be the most thermodynamically stable state. To test this hypothesis, we have carried out a series of simulations of the hard spherocylinder dimer system to directly probe the free energy difference between polar and antipolar states. We performed constant-pressure Monte Carlo simulations of periodic systems of hard bent-core molecules in the SmAP phase, using a shifted periodic boundary condition to ensure two effective layers in our system. Systems consisting of 400 bent-core molecules with an opening angle $\psi=120^\circ$ (corresponding to the opening angle present in the main class of bent-core molecules) and a length-breadth ratio $L/D=5$ for each spherocylinder were simulated at a reduced pressure $P^*=7.5$. This state point is in the middle of the SmAP phase range (see Fig. 1). Each run consists of 2×10^5 sweeps for equilibration and 4×10^6 sweeps for production.

Umbrella sampling [32] makes use of a biasing potential to measure the probability distribution of a quantity Q ,

$$P(Q) = \langle \delta(Q - Q(\mathbf{r}^N)) \rangle = \frac{1}{Z} \int dV \int d\mathbf{r}^N \delta(Q - Q(\mathbf{r}^N)) \times \exp\{-\beta[U(\mathbf{r}^N) + PV]\}, \quad (1)$$

for values of Q for which $P(Q)$ is small. Here, δ is a Dirac delta function, N is the number of particles, \mathbf{r}^N denotes the set of particle coordinates, $\beta = (k_B T)^{-1}$, where k_B is the Boltzmann's constant, T is the absolute temperature, P is the absolute pressure, and V is the volume of the system, $U(\mathbf{r}^N)$ is the potential energy, and Z is the configurational partition function. The biasing potential $U'(Q)$ is applied to constrain Q to some specified range of values. The distribution of Q in the presence of a biasing potential is

$$P'(Q) = \frac{1}{Z'} \int dV \int d\mathbf{r}^N \delta(Q - Q(\mathbf{r}^N)) \exp\{-\beta[U(\mathbf{r}^N) + U'(Q) + PV]\} = \frac{Z}{Z'} \exp[-\beta U'(Q)] P(Q), \quad (2)$$

where Z' is the partition function for the biased Hamiltonian. From this it follows that

$$P(Q) = \frac{Z'}{Z} \exp[\beta U'(Q)] P'(Q). \quad (3)$$

Thus, the distribution function $P(Q)$ can be obtained (to within a multiplicative constant) from a measurement of the biased distribution $P'(Q)$. The Gibbs free energy G as a function of Q can then be obtained (to within an additive constant) from [33]

$$G(Q) = -k_B T \ln[P(Q)]. \quad (4)$$

By piecing together distributions measured using a number of biasing potentials, it is possible to construct $P(Q)$ [and thus $G(Q)$] over any specified range of Q . Histograms obtained with individual biasing potentials are combined to minimize the variance in the overall $P(Q)$ using the weighted histogram analysis method [34].

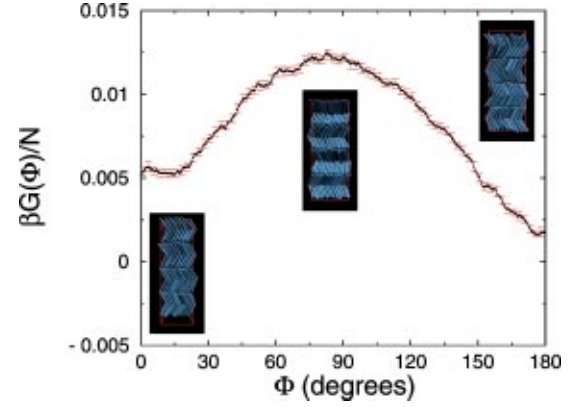


FIG. 5. (Color online only) Free energy of SmAP phase as a function of Φ for bent-core molecules with an opening angle $\psi = 120^\circ$, $L/D = 5$ at $P^* = 7.5$. Snapshots from this series of simulations are also shown, for $\Phi_0 = 0^\circ$ (left), $\Phi_0 = 90^\circ$ (center), and $\Phi_0 = 180^\circ$ (right).

To measure the free energy difference of the hard bent-core system as a function of polar angle Φ between the projection of the polar order parameters \mathbf{p}_1 and \mathbf{p}_2 of the two layers in the plane of the smectic layer, we constrain the polar angle with a harmonic biasing potential,

$$U'(\Phi) = \frac{1}{2} k_\Phi (\Phi - \Phi_0)^2, \quad (5)$$

where $\Phi = \arccos(\mathbf{p}_1 \cdot \mathbf{p}_2 / |\mathbf{p}_1| |\mathbf{p}_2|)$ and \mathbf{p}_i is the projection of the polar order parameter \mathbf{m}_i into the plane of layer i . Choosing $\Phi_0 = 0$ biases the system toward a polar state and $\Phi_0 = \pi$ biases the system toward an antipolar state.

In Fig. 5 we show the reduced Gibbs free energy, $\beta G/N$ as a function of Φ . Also shown are several representative configurations from this series of simulations. It is important to note that the biasing potential acts on the overall polar order parameter of each layer, not on individual molecules, and so is minimally perturbative. In particular, the biasing potential does not, *a priori*, suppress polar order fluctuations.

As anticipated, we measure a small but significant difference in free energy between polar and antipolar states. The antipolar state has lower free energy than the polar state consistent with the simple sawtooth model. The free energy difference between polar and antipolar states is $\beta \Delta G/N = \beta(G_F - G_A)/N = 0.0035 \pm 0.0002$. As the volume does not vary significantly with Φ , it is clear that the measured variation in free energy is entropic in origin, consistent with the sawtooth model. Based on these calculations as well as on the calculations of the simple spherocylinder model, we anticipate that the most stable SmAP phase is the antipolar state (SmAP_A), although similar studies for a wider range of opening angles ψ and reduced pressures P^* are needed.

IV. CONCLUSIONS

The spherocylinder dimer model exhibits rich phase behavior, including polar and nonpolar crystal, columnar, polar and nonpolar smectic, nematic and isotropic phases. In particular, the existence and range of stability of the nematic phase are in good agreement with the behavior of the new

class of bent-core molecules, while the stability of the non-polar smectic *A* phase is in qualitative agreement with experiments. In addition, our model predicts the existence and stability of a polar smectic *A* phase for $\psi < 167^\circ$ and free energy calculations show that the most thermodynamically stable polar smectic state is the SmAP_A . The range of stability of polar smectic phases in our model is also in general qualitative agreement with experiments. However, no spontaneous chiral symmetry breaking is observed, and a simple extension of the present model, taking into account the important steric role played by the flexible LC tails in the formation of tilted smectic phases, is currently under investigation. Our model indicates that there is no intrinsic coupling between polar symmetry breaking and chiral symmetry breaking, and that the latter is not directly related to the bent-core shape of the molecules.

Finally, it is of interest to consider the effect of varying the length-to-breadth ratio L/D on the properties of the present model. The chirality of bent-core materials appears to be a consequence of simultaneous polar and chiral symmetry breaking. It is unlikely that the simple spherocylinder dimer model exhibits tilted smectic phases for any value of L/D , based on the observation that the simple hard spherocylinder system does not exhibit tilted smectic phases for any L/D [17,18].

It is worth noting that an earlier study of hard spherocylinder dimers [20] for smaller L/D also did not find any tilted smectic phases. We, therefore, expect that the appearance of tilted smectic phases (and hence structural chirality) requires additional interactions or a more complex molecular shape. As is clear from simulations of the hard biaxial ellipsoid system [35,36], a biaxial nematic phase requires a highly biaxial molecular shape, which is achieved in the hard spherocylinder dimer case for large L/D and for a specific range of values of opening angle, as has been predicted theoretically [16]. The biaxial nematic phase is predicted to appear between the N_+ (prolate nematic) and N_- (oblate nematic) phases and arises for a molecular shape that is in some sense simultaneously rodlike and platelike owing to its biaxiality. Thus, it remains a distinct possibility that a biaxial nematic phase is stable for larger L/D in the hard spherocylinder dimer system.

ACKNOWLEDGMENT

This work was supported by NSF MRSEC Grant No. DMR 98-09555.

-
- [1] M.C. Maugin, *Bull. Soc. Fr. Mineral.* **34**, 71 (1911); C.W. Oseen, *Trans. Faraday Soc.* **29**, 883 (1933); H. de Vries, *Acta Crystallogr.* **4**, 219 (1951).
- [2] D. Armitage and F.P. Price, *J. Phys. (France)* **36**, C1 (1975).
- [3] R.B. Meyer, L. Liebert, L. Strzelecki, and P. Keller, *J. Phys. (France)* **36**, L69 (1975).
- [4] A. Fukuda, Y. Takanashi, T. Isozaki, K. Ishikawa, and H. Takezoe, *J. Mater. Chem.* **4**, 997 (1994).
- [5] S.R. Renn and T.C. Lubensky, *Phys. Rev. A* **38**, 2132 (1988).
- [6] T. Niori, T. Sekine, J. Watanabe, T. Furukawa, and H. Takezoe, *J. Mater. Chem.* **6**, 1231 (1996).
- [7] D.R. Link, G. Natale, R. Shao, J.E. MacLennan, N.A. Clark, E. K orblova, and D.M. Walba, *Science* **278**, 1924 (1997).
- [8] F. Kentischer, R. MacDonald, P. Warnick, and G. Heppke, *Liq. Cryst.* **25**, 341 (1998).
- [9] F. Araoka, B. Park, Y. Kinoshita, K. Ishikawa, H. Takezoe, J. Thisayukta, and J. Watanabe, *Jpn. J. Appl. Phys., Part 1* **38**, 3526 (1998).
- [10] V.L. Lorman and B. Mettout, *Phys. Rev. Lett.* **82**, 940 (1999).
- [11] P. Tol dano, O.G. Martins, and A. Figueiredo Neto, *Phys. Rev. E* **62**, 5143 (2000).
- [12] A. Eremin, S. Diele, G. Pelzl, H. N adasi, W. Weissflog, J. Salfetnikova, and H. Kresse, *Phys. Rev. E* **64**, 051707 (2001).
- [13] I. Wirth, S. Diele, A. Eremin, G. Pelzl, S. Grande, L. Kovalenko, N. Panceko, and W. Weissflog, *J. Mater. Chem.* **11**, 1642 (2001).
- [14] D. Shen, S. Diele, G. Pezl, I. Wirth, and C. Tschierske, *J. Mater. Chem.* **9**, 661 (2001).
- [15] S.K. Kumar (private communication).
- [16] P.I.C. Teixeira, A.J. Masters, and B.M. Mulder, *Mol. Cryst. Liq. Cryst.* **323**, 167 (1999).
- [17] S.C. McGrother, D.C. Williamson, and G. Jackson, *J. Chem. Phys.* **104**, 6755 (1996).
- [18] P. Bolhuis and D. Frenkel, *J. Chem. Phys.* **106**, 666 (1997).
- [19] L. Onsager, *Ann. N.Y. Acad. Sci.* **51**, 627 (1949).
- [20] P.J. Camp, M.P. Allen, and A.J. Masters, *J. Chem. Phys.* **111**, 9871 (1999).
- [21] J. Xu, R.L.B. Selinger, J.V. Selinger, and R. Shashidhar, *J. Chem. Phys.* **115**, 4333 (2001).
- [22] R. Memmer, *Liq. Cryst.* **29**, 483 (2002).
- [23] T.J. Dingemans and E.T. Samulski, *Liq. Cryst.* **27**, 131 (2000).
- [24] W. Weissflog, L. Kovalenko, I. Wirth, S. Diele, G. Pelzl, H. Schmalfluss, and H. Kresse, *Liq. Cryst.* **27**, 677 (2000).
- [25] D.A. Olson, X.F. Han, A. Cady, W. Weissflog, and C.C. Huang, *Phys. Rev. Lett.* **88**, 085504 (2002).
- [26] M.P. Allen and D.J. Tildesley, *Computer Simulation of Liquids* (Oxford University Press, Oxford, London, 1987).
- [27] W.G. Jang, M.A. Glaser, C.S. Park, K.H. Kim, Y. Lansac, and N.A. Clark, *Phys. Rev. E* **64**, 051712 (2001).
- [28] M.A. Glaser, Y. Lansac, M. Nendel, W.G. Jang, D.M. Walba, and N.A. Clark (unpublished).
- [29] M.A. Glaser, N.A. Clark, M. Nendel, and D.M. Walba, in *Abstracts of the Seventh International Conference on Ferroelectric Liquid Crystals*, edited by W. Hase, Darmstadt, Germany, 1999 (unpublished).
- [30] Y. Takanashi, A. Ikeda, H. Takezoe, and A. Fukuda, *Phys. Rev. E* **51**, 400 (1995).
- [31] M.A. Glaser, and N.A. Clark, *Phys. Rev. E* (to be published).
- [32] G.M. Torrie and J.P. Valleau, *Chem. Phys. Lett.* **28**, 578 (1974).
- [33] L.D. Landau and E.M. Lifshitz, *Statistical Physics*, 3rd ed. (Pergamon, London, 1980).
- [34] A.M. Ferrenberg and R.H. Swendsen, *Phys. Rev. Lett.* **63**, 1195 (1989).
- [35] M.P. Allen, *Liq. Cryst.* **8**, 499 (1990).
- [36] P.J. Camp and M.P. Allen, *J. Chem. Phys.* **106**, 6681 (1997).